Distribution of DNA Strand Breaks Produced by Iodine-123 and Indium-111 in Synthetic Oligodeoxynucleotides

Valeri N. Karamychev, Michael W. Reed, Ronald D. Neumann and Igor G. Panyutin

From the Department of Nuclear Medicine, Warren G. Magnuson Clinical Center, National Institutes of Health, Bethesda (V. N. Karamychev, R. D. Neumann, I. G. Panyutin) and Epoch Pharmaceuticals, Redmond, WA (M. W. Reed) USA

Correspondence to: Dr Igor G. Panyutin, National Institutes of Health, 10 Center Dr., Room 1C401, Bethesda, MD 20854-1180, USA. Tel: +1 301 496 8308. E-mail: igorp@helix.nih.gov

Acta Oncologica Vol. 39, No. 6, pp. 687–692, 2000

Antigene radiotherapy, a procedure based on delivery of short-range Auger-electron-emitting radioisotopes to target genes via sequence-specific triplex-forming oligonucleotides, has been successfully demonstrated in vitro using the well-studied radionuclide ^{125}I. To proceed with in vivo trials, Auger electron emitters with shorter half-lives than ^{125}I are required. Here we report a study of the efficiency and distribution of sequence-specific DNA strand breaks produced by decay of ^{123}I and ^{111}In. ^{123}I and ^{111}In were introduced into triplex- and duplex-forming oligodeoxyribonucleotides (ODNs) through carbohydrate linkers of various lengths. Labeling with radioiodine was performed through tributylstannylbenzamide intermediates while ^{111}In was attached via DTPA. The Auger-emitter-labeled ODNs were hybridized to a single-stranded DNA target, to form duplexes. After decay accumulation, the target DNA samples were assayed for strand breaks using a sequencing gel-electrophoresis technique. For the first time, we observed footprints of DNA strand breaks produced by ^{123}I and ^{111}In. Most of the breaks were located within 10 nucleotides from the decay site. The yield of strand breaks per decay varies; decay of ^{111}In breaks DNA almost 10 times more effectively than decay of ^{123}I. Both ^{123}I and ^{111}In are less effective in breaking DNA strands than ^{125}I, which reflects the higher total energy of the Auger decay process of ^{125}I.

Received 11 August 1999
Accepted 18 May 2000

Targeting of Auger-electron-emitting radioisotopes to specific sites in the genome could potentially result in antigene radiotherapy (1). Decay of the Auger emitters causes DNA breaks in the target gene, leading, under certain conditions, to its inactivation. For delivery of Auger emitters to targets in the genome, we proposed the use of triplex-forming oligonucleotides (TFO) that can bind to the DNA duplex sequence, specifically by forming so-called Hoogsteen bonds with Watson-Crick base pairs (bp) (2).

In in vitro studies using ^{125}I, we demonstrated that TFO could deliver radioiodine to specific targets in cellular DNA in order to inactivate genes and/or kill the cells containing the target sequences (3–5). Decay of ^{125}I delivered by TFO resulted in strand breaks in both strands of the target DNA, with an efficiency ranging from 0.4 to 0.8 breaks/decay (5). Higher efficiency could be achieved by multiple labeling of TFO with radionuclides. Breaks were confined to the triplex target sequence, and 90% of the sequence-specific breaks are located within 10 bp around the decay site (3). The specificity of TFO was shown to be high enough selectively to break genomic DNA in a target located in a single-copy human HPRT gene (4). A liposome delivery system has been developed effectively to deliver radiolabeled TFO into the cell nucleus (6). The radiotoxicity of TFO delivered into the cell nucleus as measured by a clonogenic assay was 300 times less than that of DNA-incorporated ^{125}I-UdR (6).

We have also shown that the fine structure of the DNA damage produced by decay of an Auger electron emitter depends on local DNA conformation, and therefore by analyzing the DNA damage, one can obtain information on the structure of DNA in nucleoprotein complexes both in vitro and in vivo (5). Based on this principle, a new method of radioprobing of DNA-protein complexes has been demonstrated in several model systems (7).

The relatively long half-life of ^{125}I (60 days) impedes the use of this radionuclide for in vivo trials of antigene radiotherapy. For experiments in animal models and future clinical trials, radioisotopes with half-lives comparable with the biological half-life of oligonucleotides in vivo (which is a few days) are required. Here, we tested two Auger emitters, ^{123}I and ^{111}In, with half-lives of 13.2 h and

 ISSN 0284-186X

2.8 days, respectively. These radioisotopes were previously shown to break DNA strands, presumably by the Auger effect (8, 9). Although their efficiency for DNA cleavage and the resultant distribution of breaks which are important characterictics for antigene radiotherapy trials are not known. We measured these characteristics by controlled sequence-specific delivery of ^{123}I and ^{111}In to the target DNA via complementary oligonucleotides.

MATERIAL AND METHODS

Synthesis of oligonucleotides

Oligonucleotides were synthesized on an ABI-394 DNA synthesizer (PE Applied Biosystems) and purified as described by Karamychev et al. (10). The structure and sequence of the amine-modified oligonucleotides NH_2-ODN-1 are shown in Fig. 1A. The 3′-hexanol modification was introduced into ODN-1 by means of a hexanol-modified controlled pore glass (CPG support (11). The 5-(3-aminopropyl)-2-deoxyuridine modification was introduced into ODN-1 using the corresponding phthalimide-protected phosphoramidite. Sn-ODN-1 was prepared by conjugation of 2,3,5,6-tetrafluorophenyl 4-tri(n-butyl)stannylbenzoate with NH_2-ODN-1, as described by Reed et al. (11).

Synthesis of ^{123}I-ODN-1

A solution of 1 nmol Sn-ODN-1 in 10 μL of 0.1 M borate buffer (pH 8.5) was added to 5.2 mCi (180 pmol, 286 000 Ci/mmol) of Na^{123}I (MDS Nordion) in 25 μL of 0.1 M borate buffer (pH 8.5) and 10 μg (44 nmol) chloramine T

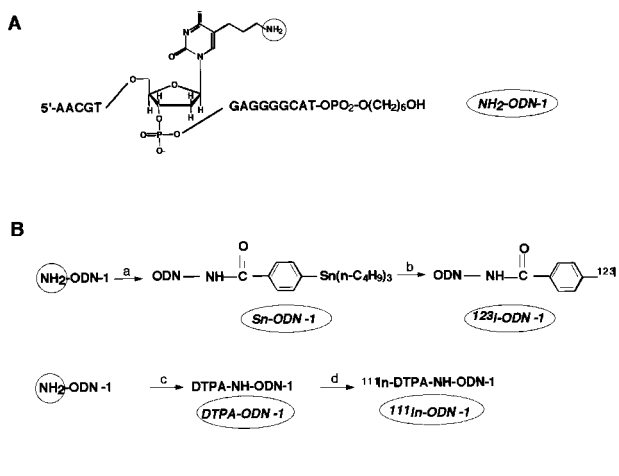

Fig. 1. A. Sequence of amine-modified oligonucleotide used for the synthesis of ^{111}In-ODN-1 or ^{123}I-ODN-1. B. Scheme for synthesis ^{123}I-ODN-1 and ^{111}In-ODN-1. Reagents: (a) 4-(tri-n-butylstannyl)benzoate, TFP ester, triethylamine, DMSO, (b) Na^{123}I, chloramine T, (c) cDTPA, DTPA, (d) $^{111}InCl_3$. C. The sequence of the duplexes. Y indicates position of labeled residues.

in 10 μL water. After 5 min, the reaction was quenched with 10 μL sodium bisulfite (10 mg/ml). The purification was done by reverse phase HPLC using LC-1 050 (Hewlett Packard) equipped with γ-RAM detector (IN/US). The retention time of ^{123}I-ODN-1 was verified by injection of non-radioactive ^{127}I-ODN-1. HPLC was performed on a 150× 4.6 mm C18 column (PRP-1 Hamilton) using a 5–85% gradient of acetonitrile in 0.1 M triethylammonium acetate (pH 7.5). The radioactive peak corresponding to the product (retention time 12.6 min, 480 μCi, 1.5 ml) was collected and lyophilized in a SpeedVac Concentrator (ATR, Rockville, USA). The sample was dissolved in 10 μL TE buffer.

Synthesis of ^{111}In-ODN-1

Conjugation of DTPA with oligonucleotides. The solutions of NH_2-ODN-1 (245 μM) were prepared in 0.5 M sodium bicarbonate (pH 8.4). To these solutions, fresh cyclic DTPA dianhydride (cDTPAA) solution (98.2 mg/ml, 0.28 mmol/ml) prepared in dry DMSO was added in three equal portions at 15-min intervals. The conjugation reaction was continued for 15 min after the last portion of the cDTPAA solution was added. The total concentration of cDTPAA was 1 260-fold in excess of the concentration of ODNs. The DTPA-conjugated ODN was then purified with spin G-50 columns (5 prime–3 prime Inc., Boulder, CO) prewashed with 0.2 M sodium acetate/0.02 M sodium citrate buffer, pH 4.5. The spin column chromatography was repeated several times until free DTPA was completely removed. The concentration of the purified DTPA-ODN conjugate was determined by UV spectroscopy (Hewlett Packard Co., Gloucester, VA). To determine the percentage of ODN conjugated to DTPA, a small fraction of DTPA-ODN conjugate was labeled with [γ-^{32}P]-ATP using T4 polynucleotide kinase (New England Biolabs) following the manufacturer's protocol and analyzed by denaturing polyacrylamide gel electrophoresis (PAGE). The gel was fixed in 10% acetic acid and then dried. The intensity of the bands corresponding to the ^{32}P-ODN and ^{32}P-DTPA-ODN was measured with a BAS 1500 BioImaging Analyzer (FUJI).

^{111}In labeling DTPA-conjugated oligonucleotides. An aliquot (1–4 μL) of this conjugate (1.03–4.12 μM) was then radiolabeled with a 15-fold molar excess of ^{111}In chloride (0.7–2.8 mCi, 15.5–62 pmol in 2.5–10 μL 0.05 M HCl) for one hour at room temperature. The pH of the solutions was adjusted to 4.5 by adding 2 M sodium acetate when necessary. The molar excess of free ^{111}In ion was then quenched by adding 5 mM DTPA and incubating for 10 min. The ^{111}In labeling yield determined by reverse-phase (Rp) TLC (Uniplate, RPS-F, 5× 20 cm, Analtech Inc., Newark, DE, eluate 10 mM sodium phosphate (pH 6.7)) and by size exclusion HPLC equipped with a Supelco G2000SW column and an on-line flow radioactivity detector (Bioscan Inc., Washington, DC). The ra-

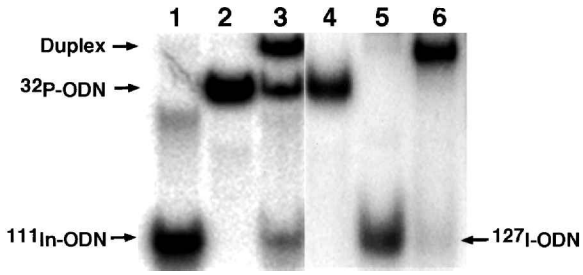

Fig. 2. Analysis of duplex formation between ^{111}In-ODN-1 or control ^{127}I-ODN-1 and ^{32}P-ODN-2 in non-denaturing PAGE. Lane 1, ^{111}In-ODN-1. Lane 2 and 4, ^{32}P-ODN-2. Lane 3, duplex ^{111}In-ODN-1/^{32}P-ODN-2. Lane 5, ^{32}P-[^{127}I-ODN-1]. Lane 6, duplex (^{32}P-[^{127}I-ODN-1]/^{32}P-ODN-2).

dioactivity on Rp-TLC was scanned with a Bioscan System 300 Imaging Scanner detector (Bioscan Inc., Washington, DC). The radioactivity peaks corresponding to ^{111}In-DTPA-ODNs and ^{111}In-DTPA were scraped off the TLC plate and counted in a gamma counter (Packard Co., Downers Grove, IL). The remaining ^{111}In-labeled products were subjected to the spin column chromatography until ^{111}In-DTPA was completely removed. The radiochemical purity of the products was confirmed by Rp-TLC and size exclusion HPLC, described above.

Duplex preparation and breaks analysis

The 42-mer target (ODN-2) was labeled with [γ-^{32}P]-ATP using T4 polynucleotide kinase (New England Biolabs) following the manufacturer's protocol. The product was purified on a MicroSpin G-50 column (Pharmacisa, NJ) and its final concentration was estimated to be 200 nM. To form ^{111}In-duplex, 0.25 pmol (1.25 µL) of ^{32}P-ODN-2 and 24 µL (15 µCi, 0.65 pmol) ^{111}In-ODN-1 was annealed at 37°C for 10 min in 1× STE buffer (50 mM Tris HCl, pH 7.5, 1 mM EDTA, 150 mM NaCl) followed by slow cooling to 20°C. To form ^{123}I-duplex, 0.25 pmol (1.25 µL) of ^{32}P-ODN-2 and 1.5 µl (70 µCi, 0.29 pmol) ^{123}I-ODN-1 was annealed at 37°C for 10 min in 10 µl 1× STE buffer (50 mM Tris HCl, pH 7.5, 1 mM EDTA, 150 mM NaCl) followed by slow cooling to 20°C.

Formation of the duplexes was confirmed in 20% non-denaturing PAGE. In the case of ^{123}I, because of a limited amount of the ^{123}I-ODN-1, as a control for duplex formation we used an equivalent concentration of ^{127}I-ODN-1 labeled with ^{32}P for visualization. After 10 days the duplex samples were analyzed for fragmentation of the target by 12% denaturing PAGE. Sequencing reactions were performed as described by Panyutin et al. (12). The gel was fixed in 10% acetic acid and dried. The bands corresponding to the breaks in ^{32}P-ODN-2 were measured with a BAS 1500 BioImaging Analyzer.

RESULTS

Oligonucleotide conjugation and labeling with ^{123}I

To synthesize ^{123}I-ODN-1, we used an approach originally developed for synthesis of ^{125}I-ODN (10, 11). The amine-modified ODN was conjugated with an aryl group and then iodinated by a halogenation/destannylation reaction (Fig. 1B). The reaction conditions and the yield of the ^{123}I-ODN-1 were similar to those described for the synthesis of ^{125}I-ODN-1 (11). ^{123}I-ODN-1 was readily purified from lipophilic Sn-ODN-1 and unreacted ^{123}I by reverse phase HPLC. Based on HPLC analysis and control experiments with ^{125}I iodination of ^{125}I-ODN-1, we assumed that 100% ODN-1 was labeled with ^{123}I.

Oligonucleotide conjugation and labeling with ^{111}In

The amine-modified ODN was conjugated with the cyclic anhydride of DTPA, as has been described by other workers (13, 14) for radiolabeling with ^{111}In using routine procedures for antibody labeling. To obtain ^{111}In-DTPA-NH-ODN with maximum specific activity, a 15-fold molar excess of ^{111}In chloride was added to the DTPA-NH-ODN solution. The excess of free ^{111}In ion was quenched by adding DTPA and was removed by several repeated gel filtration chromatographies. PAGE analysis of ^{111}In-DTPA-NH-ODN-1 is shown in Fig. 2, lane 1. We believe that the lower band is a product of ^{111}In incorporation into single-DTPA-conjugated ODNs, while the upper band results from ^{111}In incorporation into double DTPA-conjugated ODNs. The radiochemical purity of the products was confirmed by Rp-TLC, size exclusion HPLC and denaturing PAGE, as described in the Material and Methods. The measured specific activity of ^{111}In- ODN-1 was 1.6×10^7 Ci/mol, corresponding to 36% incorporation of ^{111}In into ODN-1.

Breaks in the complementary strand of a duplex

The ^{111}In-ODN-1 or control ^{127}I-ODN-1 (Fig. 1A, B) was annealed to complementary ODN-2 to form a duplex (Fig. 1C). The ODN-2 was 5′-end labeled with ^{32}P for the subsequent breaks analysis in denaturing PAGE. The non-denaturing PAGE analysis of the sample revealed that 85% of the ^{32}P-ODN-2 formed a duplex with ^{111}In-ODN-1 (Fig. 2, line 3) and 98% of the ^{32}P-ODN-2 formed duplex with control ^{127}I-ODN-1 (Fig. 2, line 6). The duplexes ^{111}In-ODN-1/^{32}P-ODN-2 and ^{123}I-ODN-1/^{32}P-ODN-2 were frozen and kept at -70°C for decay accumulation.

After 12 days of storage, the samples were analyzed for fragmentation by 12% denaturing PAGE, as shown in Fig. 3. The location of the bands in relation to the sequence of the ODN-2 was determined by comparison with the Maxam–Gilbert G-sequencing lane (lanes 4, 5). Therefore, a break at a given position means the complete removal of the corresponding base. Bands corresponding to the shorter fragments as a result of the breaks are bracketed

(Fig. 3, lanes 2, 6). The intensities of the bands were measured and, after subtraction of the corresponding areas in the blank control (lane 3), expressed as a percentage of the total radioactivity in the lanes including the top band of undamaged fragments. These values are termed frequencies of breaks (F_i). The total frequency (F) of ^{111}In (or ^{123}I) decay-induced cleavage of ^{32}P-ODN-2 calculated as the sum of the frequencies of breaks corresponding to individual bases (F_i) was 13.6% for the ^{111}In-duplex and 3.3% for the ^{123}I-duplex.

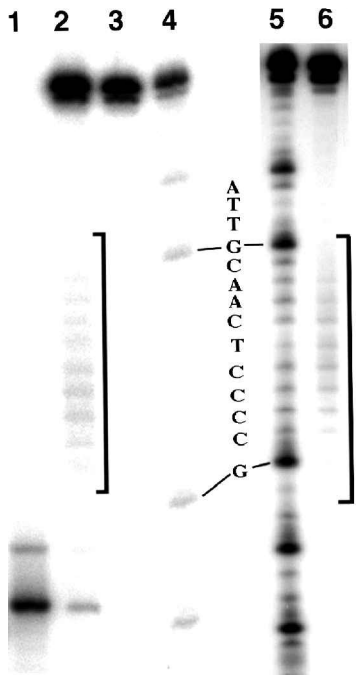

Fig. 3. Analysis of DNA breaks in 12% denaturing PAGE. Lanes: 1) ^{111}In-ODN-1, 2) duplex ^{111}In-ODN-1/^{32}P-ODN-2, 3) ^{32}P-ODN-2, 4) Maxam–Gilbert 'G' sequencing line of the ^{32}P-ODN-2, 5) Maxam–Gilbert 'G' sequencing line of the ^{32}P-ODN-2, 6) duplex ^{123}I-ODN-1/^{32}P-ODN-2. Fragments resulting from DNA breaks are bracketed.

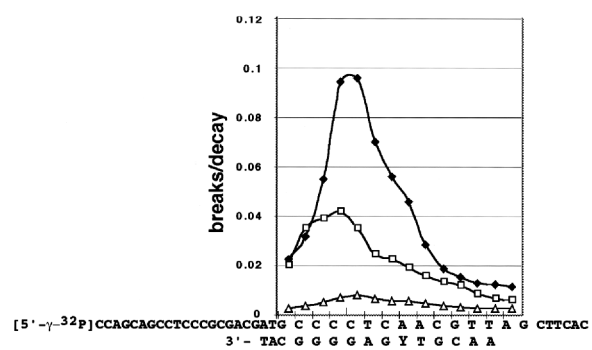

Fig. 4. Distribution and relative intensity of breaks at individual bases of ^{32}P-ODN-2 produced by ^{125}I-NH-ODN-1 (■), ^{111}In-DTPA-1 (□), ^{123}I-ODN-1 (△). Y indicates position of labeled residue.

Table 1

The yield of DNA breaks per decay of ^{123}I, ^{111}In and ^{125}I

Isotope	Linker	Linker length (Å)	Breaks/decay
^{123}I	C-3	11.3	0.03
^{111}In	C-3	11.3	0.38
^{125}I	C-3	11.3	0.66[a]
^{125}I	C-6	15.3	0.34[a]
^{125}I	None	Attached to C5 of cytosine	0.80[b]

[a] Data from (10).
[b] Data from (7).

The fraction of isotope that decayed in N days can be calculated as $1-2^{-N/T1/2}$, where $T_{1/2}$ is the half-life of the isotope ($T_{1/2} = 2.8$ days for ^{111}In and $T\phi_{1/2} = 13.2$ h for ^{123}I). Thus, after n = 12 days 89.5% of the ^{111}In and nearly 100% of the ^{123}I decayed. Taking into account that efficiency of incorporation of ^{111}In into ODN-1 was 36% and only 85% of ODN-2 was bound to ^{111}In-ODN-1, we calculated the yield of strand breaks per decay of ^{111}In as $B = 13.6/(0.895\times\ 0.36\times\ 85) = 0.35$. The estimated efficiency of incorporation of ^{123}I into ODN-1 was 100% and 98% of ODN-2 was bound to ^{123}I -ODN-1. Therefore, the yield of strand breaks per decay of ^{123}I is $B = 3.3/(1\times\ 1\times\ 98) = 0.034$.

The bar graph in Fig. 4 shows the yields of single strand breaks per decay of ^{111}In and ^{123}I for individual bases (B_i) of ^{32}P-ODN-2 (calculated as $B_i = F_i\times\ B/F$). The data for ^{125}I-duplex, bearing the same linker are from Karamychev et al. (10). The maximum of the breaks distribution is shifted four bases towards the 5′ end of the target strand from the position of the attachment of the linker (Fig. 4). The yield of strand breaks per decay of ^{111}In was nearly two times less than that of strand breaks per decay of ^{125}I and nearly 10 times more than the yield of strand breaks per decay of ^{123}I for the duplex bearing the same linker (see Table 1).

DISCUSSION

Decay of Auger electron emitters in close proximity to DNA creates a footprint of DNA strand breaks (5, 15). Analysis of the footprint gives insight into the mechanisms of DNA damage by Auger emitters. The first data on the ^{125}I-produced distribution of DNA breaks published almost 20 years ago by Martin and Haseltine (15) resulted in a burst of microdosimetry models for Auger-emitting radioisotopes. Here we present similar studies for two other Auger emitters, ^{123}I and ^{111}In. The earlier experiments showed a significant increase in efficiency of DNA strand breaks produced by decay of ^{111}In with a decrease in distance from the decay site to DNA (9). The radiotoxicity of ^{123}I-UdR expressed characteristics of high-LET-type radiation. These facts suggest that an Auger effect was involved in DNA damage by these radionuclides. Our

presentation of footprints of DNA strand breaks produced by the decay of ^{123}I and ^{111}In is the first experimental evidence that the Auger effect is the main mechanism of direct DNA damage by these radioisotopes. We obtained fine structures of localized DNA breaks, the first of the kind since the original data for ^{125}I, proving the universality of the mechanism of direct DNA damage by Auger emitters. In all the cases the breaks are highly localized, 90% are within 10 bp or one turn of the DNA double helix, and have similar distributions along the DNA strand.

Earlier we showed that the efficiency of strand breaks with ^{125}I was highly dependent on the position of radioisotope relative to DNA; in other words, on the length of the linker and the placement relative to DNA ends (see Table 1 and (10)). By combining the data obtained in this study with our previously published results we were able to compare the efficiencies of DNA breaks by ^{125}I, ^{123}I and ^{111}In attached to the same DNA fragment through the same linker. The fact that ^{111}In breaks DNA only half as effectively as ^{125}I is in good agreement with calculated total energies and numbers of Auger electrons (16). Surprisingly, the estimated number of DNA breaks per decay of ^{123}I is 20 times less than that of ^{125}I. Based on theoretical calculations and experimental data on radiotoxicity, the efficiency of DNA breakage by ^{123}I was expected to be only two times lower than that by ^{125}I, and close to that of ^{111}In.

We have two possible explanations for this discrepancy. The first explanation is a technical one; we could have overestimated the specific activity of ^{123}I-ODN-1 or, in other words, the incorporation of ^{123}I was not 100%. In our numerous experiments on Sn-ODN iodinations with ^{125}I, the specific activity based on UV spectra of the products was always close to theoretical, i.e. 100% of ODNs contained radioiodine. In the case of ^{123}I-ODN-1, UV spectra of the product could not be taken owing to their very low concentrations. Therefore, the specific activity of ^{123}I-ODN-1 was not directly measured. On the other hand, despite assurances by the supplier, the specific activity could be overestimated if ^{123}I contained a certain amount of non-radioactive iodine. The number of breaks per decay presented in the Table 1 would then be correspondingly underestimated. Similarly, discrepancies in ^{123}I-specific activity after HPLC purification of the product have been observed by others (17).

A second possible explanation is based on a suggestion that different Auger emitters have different ranges of damage. Indeed, in the experiments on radiotoxicity ^{123}I and ^{125}I were directly incorporated into DNA, whereas in our experiments they were attached through linkers. The discrepancy between the two sets of data could be explained if the damage produced by decay of ^{123}I is concentrated within a somewhat shorter range of distances than the damage produced by decay of ^{125}I. Further experiments and theoretical calculations are required to prove or disprove this explanation.

In conclusion, we developed and applied a rapid procedure for incorporation of the short-life Auger electron emitters ^{123}I and ^{111}In into ODNs, and for the first time measured the yield and distribution of direct DNA breaks produced by these radionuclides. We consider the efficiency of DNA cleavage by ^{111}In as acceptable for in vivo trials of antigene radiotherapy. For such trials ^{111}In should be attached to an ODN with a modified backbone in order to increase ODN biological stability. We plan to modulate the efficiency of DNA cleavage by varying the distances from the decay site to the DNA backbone, e.g. via attachment of various Auger emitters to oligonucleotides through ligands with different affinity to duplex DNA. These experiments may provide us with tools for antigene radiotherapies that are precise enough to permit the 'radioexcision' of faulty genes, thereby facilitating proper gene expression through a better understanding of DNA repair to perhaps promote truly corrective gene therapy.

REFERENCES

1. Panyutin IG, Neumann RD. Gene radiotherapy; gene targeted versus targeted by gene product. J Nucl Med 1998; 39: 928–9.
2. Frank-Kamenetskii MD, Mirkin SM. Triplex DNA structures. Annu Rev Biochem 1995; 64: 64–95.
3. Panyutin IG, Neumann RD. Sequence-specific DNA double-strand breaks induced by triplex forming ^{125}I-labeled oligonucleotides. Nucleic Acids Res 1994; 22: 4979–82.
4. Panyutin IG, Neumann RD. Sequence-specific DNA breaks produced by triplex-directed decay of iodine-125. Acta Oncol 1996; 35: 817–23.
5. Panyutin IG, Neumann RD. Radioprobing of DNA: distribution of DNA breaks produced by decay of ^{125}I incorporated into a triplex-forming oligonucleotide correlates with geometry of the triplex. Nucleic Acids Res 1997; 25: 883–7.
6. Sedelnikova OA, Panyutin IG, Thierry AR, Neumann RD. Radiotoxicity of iodine-125-labeled oligodeoxyribonucleotides in mammalian cells. J Nucl Med 1998; 39: 1412–8.
7. Karamychev VN, Zhurkin VB, Garges S, Neumann RD, Panyutin IG. Detecting the DNA kink in a DNA-CRP complex in solution with iodine-125 radioprobing. Nature Struct Biol 1999; 6: 747–50.
8. Makrigiorgos GM, Berman RM, Baranowska-Kortylewicz J, et al. DNA damage produced in V79 cells by DNA-incorporated iodine-123: a comparison with iodine-125. Radiat Res 1992; 129: 309–14.
9. Sahu SK, Kassis AI, Makrigiorgos GM, Baranowska-Kortylewicz J, Adelstein SJ. The effects of indium-111 decay on pBR322 DNA. Radiat Res 1995; 141: 193–8.
10. Karamychev VN, Panyutin IG, Reed MW, Neumann RD. Effect of radionuclide linker structure on DNA cleavage by ^{125}I-labeled oligonucleotides. Antisense Nucleic Acid Drug Dev 1997; 7: 549–57.
11. Reed MW, Panyutin IG, Hamlin D, Lucas DD, Wilbur DS. Synthesis of ^{125}I-labeled oligonucleotides from tributylstannylbenzamide conjugates. Bioconjug Chem 1997; 8: 238–43.

12. Panyutin IG, Wells RD. Nodule DNA in the $(GA)_{37}.(CT)_{37}$ insert in superhelical plasmids. J Biol Chem 1992; 267: 5495–501.
13. Hnatowich DJ, Winnard Jr P, Virzi F, et al. Technetium-99m labeling of DNA oligonucleotides. J Nucl Med 1994; 36: 2306–14.
14. Dewanjee MK, Ghafouripour AK, Kapadvanjwala M, et al. Noninvasive imaging of c-myc oncogene messenger RNA with indium-111-antisense probes in a mammary tumor-bearing mouse model. J Nucl Med 1994; 35: 1054–63.
15. Martin RF, Haseltine WA. Range of radiochemical damage to DNA with decay of iodine-125. Science 1981; 213: 896–8.
16. Sastry KSR, Howel RW, Rao DV, et al. Dosimetry of Auger emitters: physical and phenomenological approaches. In: Baverstock KFC, Charlton DE, eds. DNA damage by Auger emitters. London: Taylor & Francis, 1988: 27–38.
17. Dougan H, Hobbs JB, Weitz JI, Lyster DM. Synthesis and radioiodination of a stannyl oligodeoxyribonucleotide. Nucleic Acids Res 1997; 25: 2897–901.